Molecular Plant Pathology

MOLECULAR PLANT PATHOLOGY (2018) 19(6), 1364–1376 DOI: 10.1111/mpp.12620

A mutation in an exoglucanase of *Xanthomonas oryzae* pv. *oryzae*, which confers an endo mode of activity, affects bacterial virulence, but not the induction of immune responses, in rice

LAVANYA TAYI†,¶, SUSHIL KUMAR‡,¶, RAJKANWAR NATHAWAT, ASFARUL S. HAQUE§, ROSHAN V. MAKU, HITENDRA KUMAR PATEL, RAJAN SANKARANARAYANAN* AND RAMESH V. SONTI*

CSIR-Centre for Cellular and Molecular Biology, Hyderabad 500007, India

SUMMARY

Xanthomonas oryzae pv. *oryzae* (*Xoo*) causes bacterial blight, a serious disease of rice. *Xoo* secretes a repertoire of cell wall-degrading enzymes, including cellulases, xylanases and pectinases, to degrade various polysaccharide components of the rice cell wall. A secreted *Xoo* cellulase, CbsA, is not only a key virulence factor of *Xoo*, but is also a potent inducer of innate immune responses of rice. In this study, we solved the crystal structure of the catalytic domain of the CbsA protein to a resolution of 1.86 Å. The core structure of CbsA shows a central distorted TIM barrel made up of eight β strands with N- and C-terminal loops enclosing the active site, which is a characteristic structural feature of an exoglucanase. The aspartic acid at the 131st position of CbsA was predicted to be important for catalysis and was therefore mutated to alanine to study its role in the catalysis and biological functions of CbsA. Intriguingly, the D131A CbsA mutant protein displayed the enzymatic activity of a typical endoglucanase. D131A CbsA was as proficient as wild-type (Wt) CbsA in inducing rice immune responses, but was deficient in virulence-promoting activity. This indicates that the specific exoglucanase activity of the Wt CbsA protein is required for this protein to promote the growth of *Xoo* in rice.

Keywords: cellulases, endoglucanase, exoglucanase, rice, *Xanthomonas oryzae* pv. *oryzae*.

* *Correspondence*: E-mail: sonti@ccmb.res.in; sankar@ccmb.res.in

† *Present address*: Centre for Plant Molecular Biology, Osmania University, Hyderabad 500007, India.

‡ *Present address*: Institute of Life Sciences, Nalco Square, Bhuvaneshwar 751023, India.

§ *Present address*: Department of Biochemistry, McGill University, Montréal, QC H3G 0B1, Canada.

¶ These authors contributed equally to this work.

INTRODUCTION

In order to gain access to the nutrients inside host cells, an invading plant pathogen must be able to degrade the complex cell wall. Cellulose, hemicellulose and pectin form the major components of the plant cell wall. Cellulose is a linear polysaccharide composed of glucose residues linked to each other by β-1,4 glycosidic linkages. Although it is chemically a simple molecule, as it possesses only one type of monomeric sugar, it is a complex structural entity (Hon, 1994). Cellulases break down cellulose into simple monosaccharides and/or oligosaccharides. Cellulases are broadly classified into exoglucanases/cellobiohydrolases (CBHs) and endoglucanases, which differ in their architecture, substrate preference and mode of action. Exoglucanases prefer crystalline substrates, have active sites in a closed tunnel and processively remove cellobiose units from the chain ends (Teeri, 1997; Teeri *et al.*, 1998). On the other hand, endoglucanases prefer amorphous regions, have their active sites in an open cleft and make random internal cuts in the polymer (Teeri, 1997).

A number of bacterial plant pathogens belonging to the genera *Xanthomonas*, *Erwinia*, *Ralstonia*, etc., and fungal pathogens of the genera *Rhizoctonia*, *Magnaporthe*, etc., secrete cellulases. The major secreted cellulases produced by these plant pathogens have been demonstrated to be required for complete virulence of the organism (Gough *et al.*, 1988; Roberts *et al.*, 1988; Xia *et al.*, 2016). Cellulases are also potent inducers of defence responses in host tissues. For instance, cellulase treatment induces the production of salicylic acid, a defence hormone, and confers resistance to mild mottle virus attack in pepper (Sato *et al.*, 2011).

Xanthomonas oryzae pv. *oryzae* (*Xoo*) causes a serious bacterial blight disease of rice. It secretes a variety of cell wall-degrading enzymes (CWDEs), including an endoglucanase (ClsA), predicted CBH (CbsA), xylanase (XynB), lipase/esterase (LipA), pectin methyl esterase (Pmt) and polygalacturonase (PglA), to degrade the rice cell wall. Purified preparations of CbsA, ClsA and LipA are potent inducers of rice defence responses, such as callose deposition and programmed cell death. Prior treatment of rice leaves with any one of these enzymes provides enhanced resistance against subsequent infection by *Xoo* (Jha *et al.*, 2007).

Mutations in the *clsA*, *cbsA*, *lipA* and *xynB* genes have been shown to affect virulence on rice, whereas mutations in the *pmt* and *pglA* genes have minimal effects on virulence (Jha *et al.*, 2007; Rajeshwari *et al.*, 2005; Tayi *et al.*, 2016b). A mutation in the *cbsA* gene has a much greater effect on virulence than mutations in any of the other genes, suggesting that the CbsA protein is much more critical for virulence than the other *Xoo* secreted CWDEs. A correlation has been observed between the tissue specificity of bacterial pathogens of plants and the presence of a functional CbsA-like protein. In general, functional CbsA-like proteins are encoded in the genomes of xylem-dwelling pathogens, such as *Xoo*, but are either absent from, or are predicted to be non-functional in, the genomes of bacteria that multiply in the intercellular spaces of the palisade parenchymatous tissues (Ryan *et al.*, 2011). Because of the importance of this protein in the rice–*Xoo* interaction, we have chosen to solve its crystal structure with the objective of performing structure–function studies.

The crystal structures of many exoglucanases and endoglucanases of both bacterial and fungal origin have been solved. According to the CAZy classification of glycoside hydrolases (GHs), exoglucanases belong to GH families GH5, GH6, GH7, GH9 and GH48 (Cantarel *et al.*, 2009; Henrissat, 1991). The structures of GH6 exoglucanases, five from fungi and one from bacteria, have been solved. These include the Cel6A proteins of *Trichoderma reesei*, *Humicola insolens* and *Chaetomium thermophyllum*, Cel6A and Cel6C of *Coprinopsis cinereia*, and Cel6B of *Thermobifida fusca* (Liu *et al.*, 2010; Rouvinen *et al.*, 1990; Sandgren *et al.*, 2013; Tamura *et al.*, 2012; Thompson *et al.*, 2012; Varrot *et al.*, 1999a). The structures of all of these exoglucanases revealed a distorted seven-stranded α/β barrel and showed a tunnel enclosing the active site which allows for the processive style of activity shown by CBHs. The GH6 family of exoglucanases catalyses reactions via a general acid–base mechanism. In these enzymes, the catalytic acid has been identified to be an aspartic acid, but the existence of a single residue functioning as a catalytic base is unclear. It is now well accepted that, in GH6 family exoglucanases, a proton-transferring network, involving an aspartate, a serine and two water molecules, performs the function of a catalytic base via a Grotthuss mechanism (Thompson *et al.*, 2012; Vuong and Wilson, 2009).

In this study, we have solved the crystal structure of the catalytic domain of CbsA. The structural features and biochemical activities shown by CbsA confirm that it is an exoglucanase as predicted. We performed biochemical and functional characterization of a mutant CbsA protein in which the active site aspartic acid at the 131st position, which is predicted to function as a catalytic base, is converted to alanine. Interestingly, we found that this mutation (D131A) converted wild-type (Wt) CbsA, a cellulase which is an exoglucanase by structure, into an endoglucanase by activity. This gain of function by the mutant protein did not affect its ability to induce rice defence responses. However, it did not support the virulence-promoting activity of CbsA, thus indicating the essentiality of a specific exoglucanase activity in the pathogenesis of *Xoo*.

RESULTS

Domain architecture of CbsA

Bioinformatics analysis of the sequence of the CbsA protein ($\sim$56 kDa) revealed the presence of an N-terminal signal peptide of 32 amino acids, followed by a catalytic domain containing 425 amino acids with predicted exoglucanase activity and a C-terminal fibronectin type 3 domain of 109 amino acids. The catalytic domain belongs to an α/β protein fold, whereas the C-terminal domain belongs to a fibronectin fold. Based on the CAZy classification, CbsA could be classified into the GH6 family of enzymes. The secreted form of CbsA is $\sim$45 kDa and has only the catalytic domain without the C-terminal fibronectin domain. The crystallization and preliminary crystallographic studies of the catalytic domain of 425 residues have been reported previously (Kumar *et al.*, 2012).

Overall structure of CbsA

The crystal structure of the catalytic domain of CbsA (PDB ID: 5XYH) was solved to a resolution of 1.86 Å with R_{work}/R_{free} (%) values of 18.89/23.77 by the molecular replacement method using the catalytic domain of a CBH Cel6B (E3) from *T. fusca* (PDB ID: 4B4H) as the search model. The refinement statistics are presented in Table 1. The core structure of the catalytic domain of CbsA shows a central distorted β-barrel made up of eight strands. The structure shows two distinct loops: an N-terminal (Y125 to Q145) loop and a C-terminal (P406 to L428) loop, which form a tunnel enclosing the active site (Fig. 1A,B). Four conserved tryptophan residues were found to line the active site pocket of CbsA (Fig. S1, see Supporting Information). These tryptophans lining the active site pocket help to anchor the substrate, possibly by virtue of a π–π interaction with the sugar rings (Koivula *et al.*, 1996; Varrot *et al.*, 1999b). The structure also reveals the presence of two additional loops, P278–S291 and G335–G355, specific to bacterial exoglucanases, which are not found in any of the fungal CBHs (Fig. 2A).

Active site of CbsA

In CbsA, the presence of loops results in the formation of an active site tunnel spanning a length of $\sim$47.7 Å and classifies CbsA as an exoglucanase, wherein its putative catalytic activity could be to perform processive hydrolysis of crystalline substrates. In order to obtain a better understanding of the active site tunnel and to decipher the putative catalytic residues, the crystal

Table 1 Data collection and refinement statistics

PDB ID	5XYH
Data collection	
Diffraction source	Rigaku MicroMax-007 HF Cu
Wavelength (Å)	1.5418
Space group	$P2_12_12_1$
Cell parameters (Å)	$a = 46.14$, $b = 90.72$, $c = 99.78$
Resolution range (Å)*	25–1.86 (1.93–1.86)
Overall B factor from Wilson plot (Å^2)	17.3
Total observations	225 473
Unique reflections	33 848 (3169)
Completeness (%)	93.9 (89.4)
Redundancy	6.7 (5.6)
$<I/\sigma I>$	31.69 (7.75)
R_{merge} (%)	4.9 (18.3)
Refinement statistics	
Resolution (Å)	1.86
No. of reflections	33 638
R_{work}/R_{free} (%)	18.89/23.77
No. of residues	424
No. of atoms	
Protein	3212
Water	474
***B*-factors (Å^2)**	
Protein	16.15
Water	19.36
Root-mean-square deviations	
Bond lengths (Å)	0.014
Bond angles (deg)	0.87
Ramachandran plot	
Most favoured region (%)	97.16
Additionally allowed region (%)	2.84
Disallowed region (%)	0

*Values in parentheses are for the highest resolution shell.

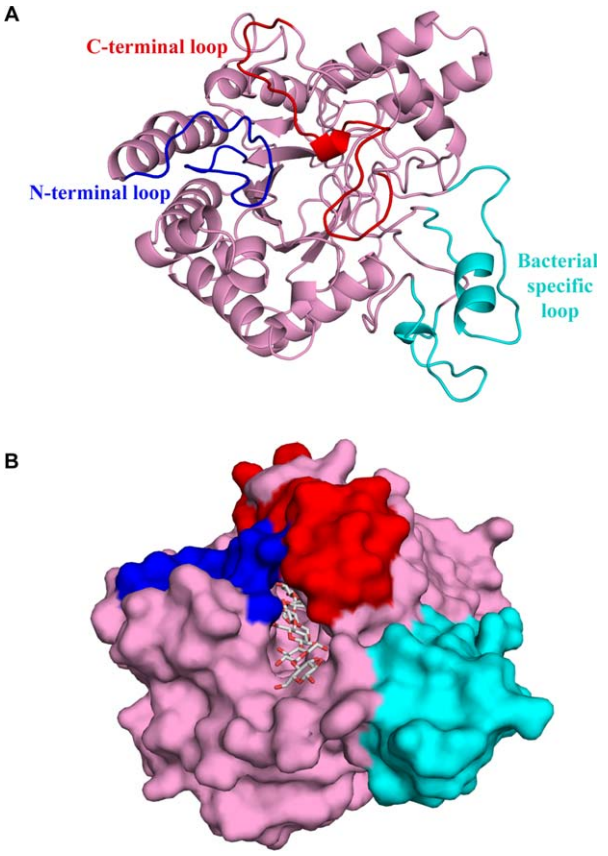

Fig. 1 Crystal structure of the catalytic domain of CbsA. (A) CbsA has a central distorted β-barrel (pink) made up of eight strands. The N- and C-terminal loops are shown in blue and red, respectively, whereas the unique loops present towards the C-terminal region are shown in cyan. (B) The CbsA structure with the modelled substrate. The surface representation of the enzyme represents a well-defined substrate-binding tunnel responsible for processive hydrolysis of the single-chain cellulose polymer. Three molecules of cellobiose were modelled from PDB ID: 4B4F.

structure of CbsA was superimposed on that of CBH Cel6B (E3) from *T. fusca* complexed with cellobiose with a root-mean-square deviation (rmsd) of 0.959 Å (PDB ID 4B4F). Subsequently, this non-hydrolysable moiety was modelled on the CbsA structure (Fig. 2B). In Cel6B of *T. fusca*, the D274 residue functions as a catalytic acid, whereas the D226 and S232 residues were found to be part of a water network which performs the role of a catalytic base (Vuong and Wilson, 2009). In the apo structure of *Xoo* CbsA, the D180, D131 and S137 residues are analogous to the D274, D226 and S232 residues of *T. fusca*, and are similarly positioned in the active site tunnel, suggesting identical roles for these residues in catalysis. Apart from the above-mentioned residues which are involved directly in acid–base catalysis, two other amino acids, which were highly conserved in all CBHs and were demonstrated to play a role in catalysis, are Y125 and D399 of *Xoo* CbsA (Fig. 2B). In *T. reesei*, the Y169 residue (the Y125 analogue) is postulated to play a role in the distortion of the glucose entering the tunnel and its conversion into a more active conformation. In addition, it has been proposed to play a role in ensuring the protonation states of acidic aspartates D175 and D221 (residues analogous to D131 and D180 of *Xoo* CbsA, respectively) which are part of the tunnel (Koivula *et al.*, 1996). Previously, the D405 residue of *H. insolens* exoglucanase Cel6A (analogous to D399 of *Xoo* CbsA) has been proposed to function as a potential catalytic base (Varrot *et al.*, 1999b). However, the role of this residue as a catalytic base is questionable on the basis of its position and environment. This particular aspartate of the active site forms a conserved salt bridge with arginine and suggests a structure-stabilizing function to this residue (Koivula *et al.*, 2002; Sandgren *et al.*, 2013). Both Y125 and D399 of *Xoo* CbsA were found to occupy identical positions and possess similar interactions with other amino acids as identified in *T. fusca* Cel6B.

D131A CbsA displays an endo mode of activity

We initiated structure–function studies of the CbsA protein by making mutations that are expected to be critical for biochemical

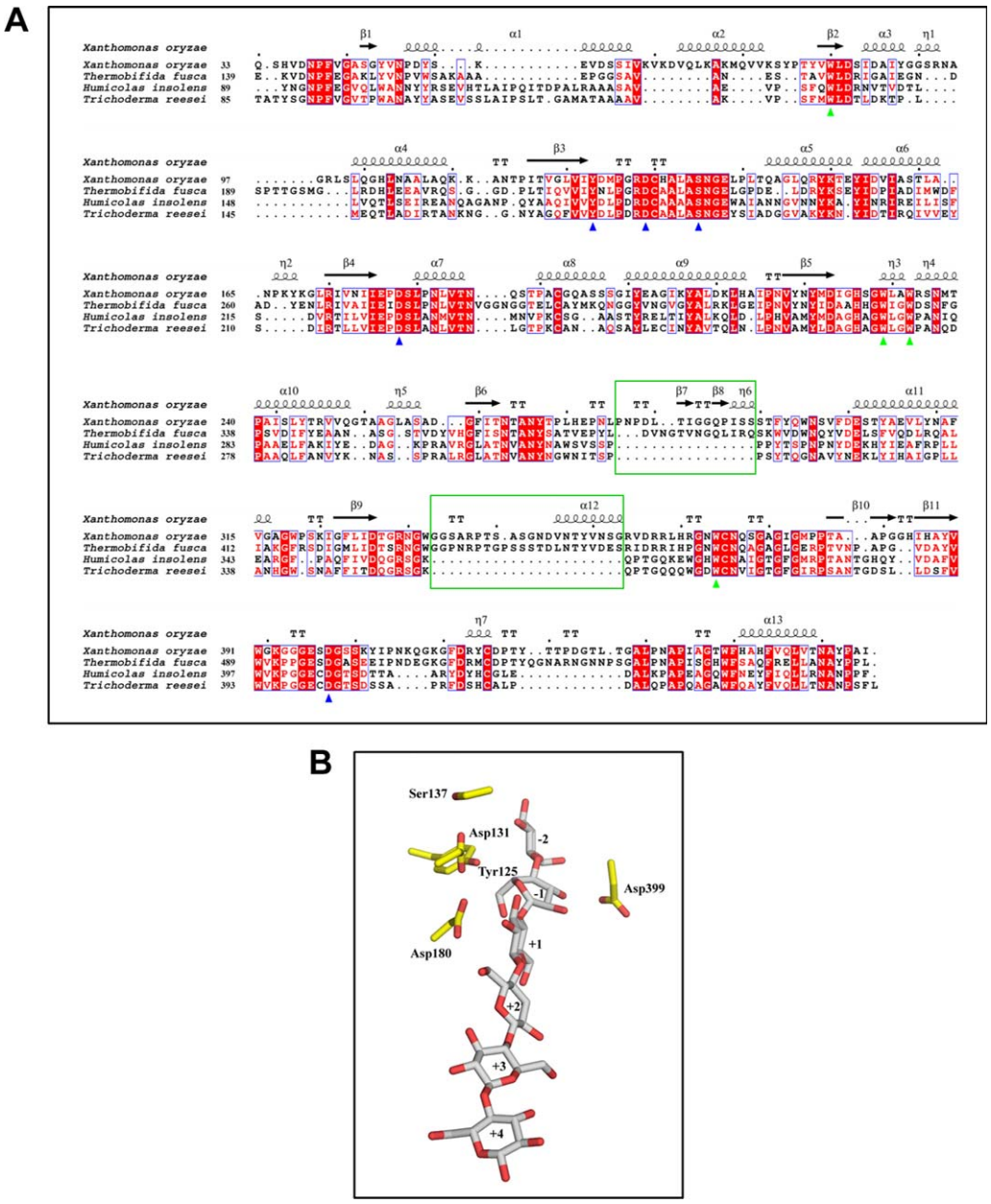

Fig. 2 Multiple sequence alignment of the CbsA catalytic domain and putative catalytic residues. (A) Multiple sequence alignment of the CbsA catalytic domain with homologous regions from other bacteria and fungi. Residues marked with a green triangle are conserved tryptophans lining the tunnel and blue triangles indicate the putative catalytic residues. The sequences of the bacterial-specific loops are enclosed in green boxes. (B) Putative catalytic residues present in close proximity to the modelled substrate. The subsites of the substrate-binding tunnel are numbered from the non-reducing end to the reducing end as −2, −1, +1, +2, +3 and +4. Residues around the active site are shown with sticks.

activity. As indicated above, the D131 residue is expected to be part of a water network that functions as a catalytic base. We made a D131A mutant of the CbsA protein and assessed the effect of the mutation on protein function. The activity of purified D131A CbsA was tested on the polysaccharide substrate carboxymethylcellulose (CMC) and on the soluble oligosaccharides cellobiose, cellotriose, cellotetraose, cellopentaose and cellohexaose. CMC is considered to be a hallmark substrate for endoglucanases because of its amorphous nature. In a CMC plate assay, *Xoo* ClsA (endoglucanase) and D131A CbsA showed a much larger halo than Wt CbsA, suggesting that CMC is cleaved better by D131A CbsA than by Wt CbsA (Fig. 3A). The specific activities of Wt CbsA and D131A CbsA on CMC were also calculated by measuring the reducing sugars released from CMC on enzyme activity (Table S1,

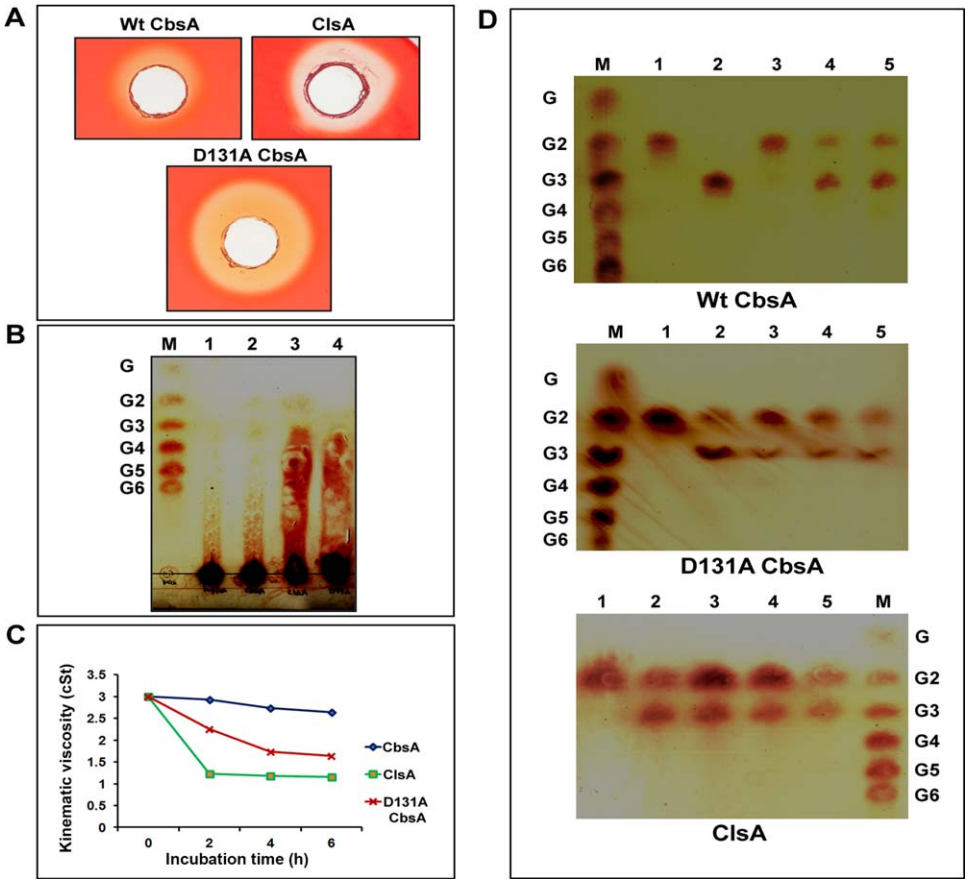

Fig. 3 D131A CbsA displays an endo mode of activity. (A) Equal amounts of purified preparations of wild-type (Wt) CbsA, D131A CbsA and ClsA proteins were added to wells in carboxymethylcellulose (CMC) plates and stained with Congo red after 36–48 h of incubation, as described in Experimental procedures. The presence of a halo around the well indicates the activity of the enzyme on CMC. (B) Separation of hydrolysed products by thin layer chromatography (TLC). The CMC substrate was incubated with buffer, Wt CbsA, D131A CbsA and ClsA, and the complete reaction mixture was spotted on a TLC sheet in the following lanes: 1, CMC + buffer; 2, CMC + Wt CbsA; 3, CMC + ClsA; 4, CMC + D131A CbsA. A mix of the oligosaccharides glucose to cellohexaose (G–G6) was loaded as a ladder in the lane labelled as M. Sugars present in the reaction mixture were separated using butanol, acetic acid and water in a 2 : 1 : 1 ratio as the mobile phase, and were detected using orcinol and sulfuric acid reagent, as described in Experimental procedures. (C) Viscometric analysis of CMC solution on activity of Wt CbsA, D131A CbsA and ClsA. The flow time of the reaction mixture containing CMC together with buffer, Wt CbsA, D131A CbsA and ClsA was measured at regular intervals using a viscosity bath maintained at a constant temperature of 37 °C. As described in Experimental procedures, the kinematic viscosity of the samples was calculated and plotted against the incubation time. (D) Activity of Wt CbsA, D131A CbsA and ClsA on soluble oligosaccharides. The oligosaccharide substrates cellobiose G2 (1), cellotriose G3 (2), cellotetraose G4 (3), cellopentaose G5 (4) and cellohexaose G6 (5) were incubated with Wt CbsA, D131A CbsA and ClsA, and the complete reaction mixture was loaded onto the TLC sheet. The sugars released were separated and detected as described in Experimental procedures. A mix of oligosaccharides (G–G6) is shown in the lane labelled as M.

see Supporting Information). The hydrolysed products of CMC obtained by the activity of Wt CbsA, D131A CbsA and ClsA were analysed by thin layer chromatography (TLC) (Fig. 3B). Wt CbsA showed very limited activity on CMC, releasing cellobiose and cellotriose in minor quantities, indicating an exo mode of activity (Fig. 3B, band 2). ClsA displayed an endo mode of activity by producing a smear emerging from the loading spot on the TLC sheet (indicative of the release of oligosaccharides of various lengths by making random cuts) (Fig. 3B, band 3). On the other hand, D131A CbsA, unlike Wt CbsA, but very similar to ClsA, released a range of oligosaccharides from CMC, as evident from the smear on the TLC sheet, suggesting random internal cleavages being made by this enzyme, similar to a typical endoglucanase (Fig. 3B, band 4). This endo mode of activity shown by D131A CbsA was further confirmed by viscometric analysis (Fig. 3C). Enzymes which make internal cuts in the substrate are expected to decrease its viscosity much more rapidly than enzymes which act from the ends of substrate molecules. ClsA reduced the viscosity of the CMC solution drastically. Wt CbsA did not decrease the viscosity of the CMC solution, even on prolonged incubation, whereas D131A CbsA decreased the viscosity at a much faster rate than Wt CbsA, but not as efficiently as ClsA (Fig. 3C). The activity of D131A CbsA on

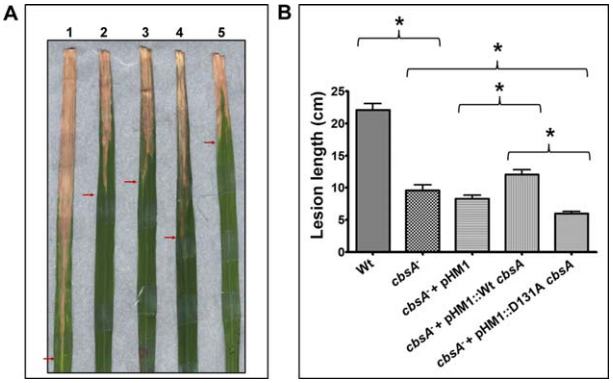

Fig. 4 Virulence phenotype of D131A mutant CbsA. (A) Rice leaves were inoculated with wild-type (Wt) *Xanthomonas oryzae* pv. *oryzae* (*Xoo*) (BXO43) (1), the *cbsA*⁻ mutant (2), the *cbsA*⁻ mutant + pHM1 (3), the *cbsA*⁻ mutant + pHM1::Wt *cbsA* (4) and the *cbsA*⁻ mutant + pHM1::D131A *cbsA* (5). At 20 days post-inoculation, the images of infected rice leaves were captured. (B) Lesion lengths were measured after 20 days. Error bars indicate the standard deviation of readings from at least 10 inoculated leaves. Similar results were obtained in independent experiments. A Student's two-tailed *t*-test for independent means was performed for the following groups: wild-type and *cbsA* mutant, mutant with empty vector (control strain), mutant expressing Wt CbsA (complemented strain) and mutant expressing D131A CbsA. *All the compared values were significantly different at the $P < 0.05$ level.

soluble oligosaccharides is also identical to ClsA (Fig. 3D). Under the conditions tested, the substrate cellobiose (G2) was not acted upon by any of the three enzymes Wt CbsA, D131A CbsA or ClsA. Wt CbsA could not act on cellotriose (G3), whereas D131A CbsA and ClsA released cellobiose (G2) from this substrate. Wt CbsA converts cellotetraose (G4) to cellobiose (G2), whereas D131A CbsA and ClsA release cellobiose (G2) and cellotriose (G3) from this substrate. Cellopentaose (G5) and cellohexaose (G6) are converted by Wt CbsA, D131A CbsA and ClsA to cellobiose (G2) and cellotriose (G3) (Fig. 3D).

D131A mutant CbsA does not support the virulence of *Xoo* on rice

The CbsA protein is an important virulence factor for *Xoo*. A *cbsA*⁻ mutant of *Xoo* is virulence deficient (Jha *et al.*, 2007). We wanted to determine whether the change in activity from the exo mode to the endo mode for D131A CbsA can still support the *in planta* virulence function of CbsA. Rice leaves were inoculated with Wt *Xoo* (BXO43), the *cbsA*⁻ mutant, the *cbsA*⁻ mutant expressing Wt CbsA and the *cbsA*⁻ mutant expressing D131A CbsA. The *cbsA*⁻ mutant strain expressing Wt CbsA (complemented strain) partially complemented the virulence deficiency of the mutant, whereas the *cbsA*⁻ mutant strain expressing D131A CbsA exhibited severe virulence deficiency (Fig. 4A). The lesions caused by the *cbsA*⁻ mutant strain expressing D131A were significantly shorter in comparison with those of the *cbsA*⁻ mutant strain expressing Wt CbsA, as well as the *cbsA*⁻ mutant strain itself (Fig. 4B). Overall, these results suggest that the altered activity caused by the D131A mutation affects the ability of this protein to promote *Xoo* virulence.

D131A CbsA is proficient in the induction of immune responses in rice

Purified preparations of *Xoo*-secreted CWDEs, such as LipA, CbsA and ClsA, have been shown to be elicitors of immune responses, e.g. callose deposition and programmed cell death, in rice tissues (Jha *et al.*, 2007). Callose deposition is a hallmark defence response shown by the host, wherein β-1,3-glucan, a polymeric substance, is deposited at the site of pathogen entry as a way of strengthening the cell wall. Programmed cell death is a host defence response in which infected cells undergo localized cell death to prevent further spread of the pathogen. We investigated whether D131A CbsA is compromised in its ability to induce plant defence responses. Infiltration of D131A CbsA into rice leaves induced callose deposits as efficiently as Wt CbsA (Fig. 5A). Similarly, treatment of rice roots with D131A CbsA induced programmed cell death as efficiently as Wt CbsA, as shown by extensive propidium iodide (PI) internalization and dispersal within the cells (Fig. 5B).

In a previous study, we have shown that the CbsA protein of *Xoo* is required for the ability of the bacterium to induce rice defence responses during infection (Tayi *et al.*, 2016a). A mutant of *Xoo* that is defective in the Type 3 secretion system (T3SS) is an inducer of rice defence responses (Jha *et al.*, 2007). A T3SS⁻ *cbsA*⁻ double mutant strain is deficient in inducing callose deposition in rice leaves, and a complemented clone expressing Wt CbsA restores to the T3SS⁻ *cbsA*⁻ mutant the ability to induce callose deposits (Tayi *et al.*, 2016a). To determine whether, *in vivo*, the altered biochemical activity of the D131A mutant protein can substitute for the activity of the Wt protein in eliciting rice innate immune responses during infection, a T3SS⁻ *cbsA*⁻ strain expressing D131A CbsA was generated and tested for its ability to induce callose deposition in rice. The T3SS⁻ *cbsA*⁻ strain expressing the D131A mutant is as efficient as the Wt complemented strain (i.e. T3SS⁻ *cbsA*⁻ expressing Wt CbsA) in the elicitation of callose deposition in rice leaves (Fig. 6A). The numbers of callose deposits induced by the T3SS⁻ *cbsA*⁻ strain expressing D131A CbsA are similar to those induced by the T3SS⁻ *cbsA*⁻ strain expressing Wt CbsA (Fig. 6B).

DISCUSSION

As part of their virulence repertoire, plant pathogens utilize a battery of enzymes, including endoglucanases and CBHs, to systematically hydrolyse the plant cell wall. *Xoo* causes the serious bacterial blight disease of rice. The CbsA protein is an important

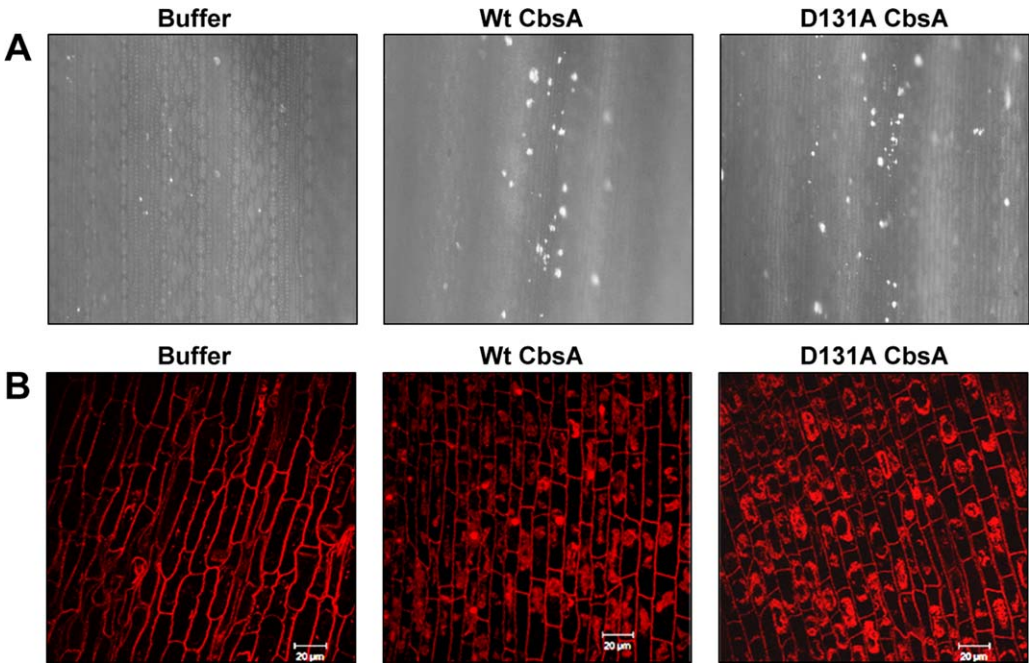

Fig. 5 D131A mutation does not affect the ability of CbsA to induce defence responses in rice tissues. (A) Callose deposition in rice leaves: 10–15-day-old rice leaves were infiltrated with 100 μL of buffer, Wt CbsA or D131A CbsA proteins of concentration 0.1 mg/mL. The leaves were subsequently treated to remove chlorophyll, stained with aniline blue and visualized under an epifluorescence microscope. Bright spots in the images are the callose deposits. (B) Programmed cell death in rice roots: roots of 2–3-day-old rice seedlings were excised and treated with buffer, Wt CbsA or D131A CbsA proteins (0.5 mg/mL) for 16 h, stained with propidium iodide (PI) and examined under a confocal microscope. Extensive internalization of PI and dispersal within the cell are indicative of programmed cell death (PCD). Scale bar measures 20 μm. The concentrations of protein used are the lowest effective concentrations for the wild type protein to elicit callose deposition and programmed cell death respectively.

virulence factor of this bacterium. In the present study, the crystal structure of the *Xoo* CbsA protein was solved to a resolution of 1.86 Å. The presence of the N- and C-terminal loops enclosing the active site confirms that this protein is an exoglucanase and that it could possibly perform processive hydrolysis of crystalline cellulose (Rouvinen *et al.*, 1990; Varrot *et al.*, 2003). In the absence of such loops, an open active site cleft would be displayed, as typically present in endoglucanases (Davies *et al.*, 2000). There are increasing lines of evidence to suggest that the substrate-enclosing loops display conformational changes on binding of the substrates and, occasionally, may facilitate endo-cleavage; thus explaining the catalytic facets of both exo- and endo-hydrolysis shown by CBHs (Varrot *et al.*, 1999b; Zou *et al.*, 1999).

Mutational studies of several CBHs have demonstrated a very important role for the aspartic acids of the active site in catalysis. Amongst these various aspartic acid residues, the analogues of *Xoo* CbsA D131 have been reported to be important for catalysis in these enzymes (Koivula *et al.*, 2002, Vuong and Wilson, 2009). Although the role of this particular aspartic acid as a catalytic base via the Grotthuss mechanism in exoglucanases is increasingly accepted, mutation of this residue to alanine still retains the enzymatic activity. Recent simulation work on *T. reesei* Cel6A has suggested that proton hopping along a short water wire is responsible for rescuing the catalytic activity of its D175A mutant protein (which is analogous to the *Xoo* D131A CbsA mutant protein) (Mayes *et al.*, 2016).

The inability of Wt CbsA or any true exoglucanase to act as efficiently as an endoglucanase on CMC is a result of their tunnel-shaped active sites and the bulky carboxymethyl substitutions on the glucose molecules of CMC which hinder the movement of the processive enzyme along the CMC molecule. The D131A CbsA enzyme showed greater activity than the Wt CbsA on CMC, as revealed by the CMC plate assay as well as specific activity calculations. The mutant enzyme also decreased the viscosity of CMC solution much more quickly than Wt CbsA, although not as efficiently as the typical endoglucanase, ClsA. These results clearly indicate that the mutant enzyme has attained the endo mode of activity. Vuong and Wilson (2009) have made similar observations regarding activity on CMC for the analogous mutant protein D226A from *T. fusca* Cel6B. Vuong and Wilson (2009) explained that the internal cleavage of CMC by D226A may be caused by the local changes brought about by replacing aspartic acid with alanine. A smaller side chain of alanine may allow the modified glucose residues of CMC to fit into the active site, enabling the mutant enzyme to move along a CMC molecule smoothly until a group of unmodified glucose residues is found to carry out internal

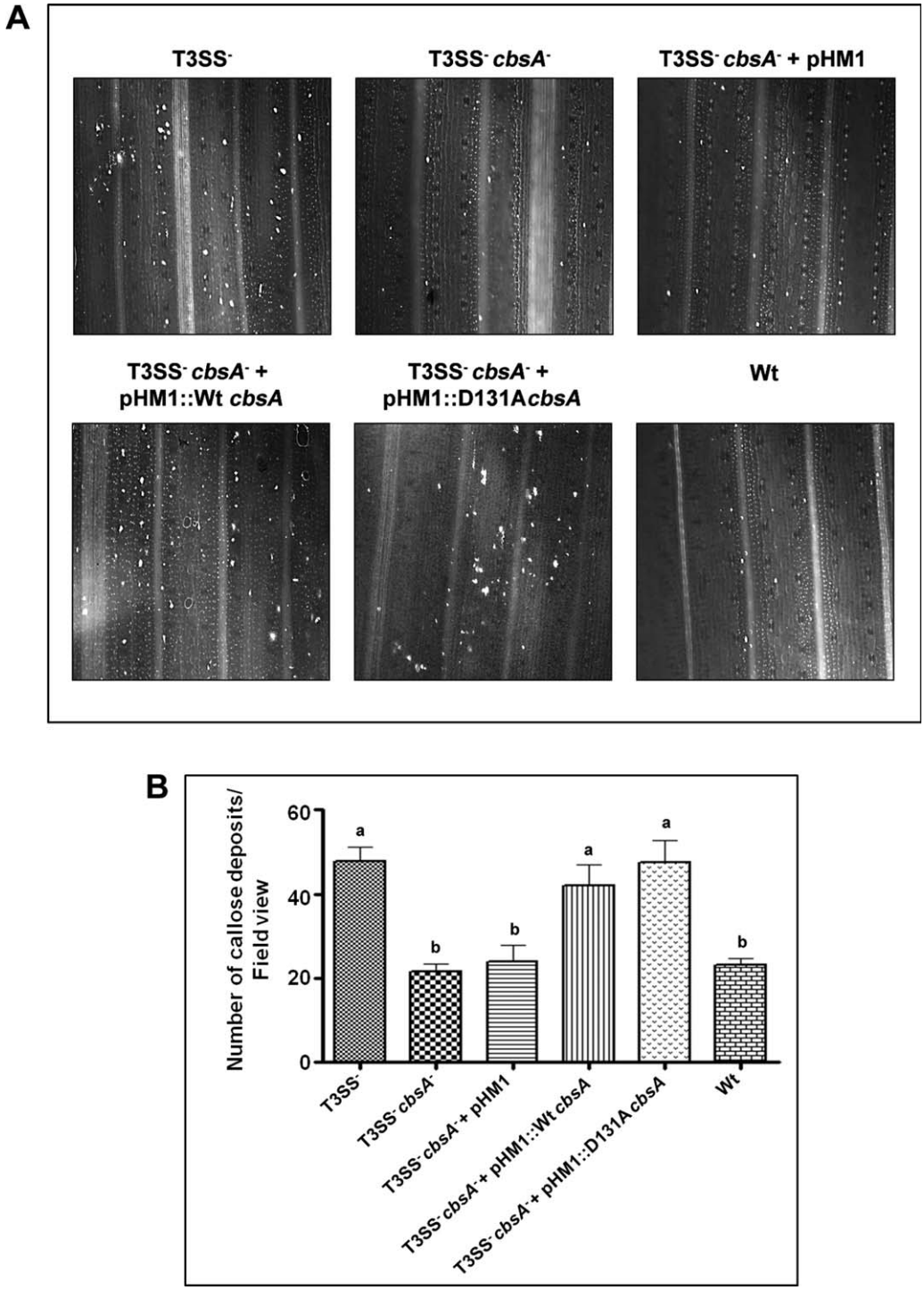

Fig. 6 D131A CbsA is as efficient as the wild-type (Wt) protein in the induction of callose deposition in rice leaves *in vivo*. (A) Ten- to 15-day-old rice leaves were infiltrated with one of the following strains of *Xanthomonas oryzae* pv. *oryzae*: T3SS⁻ mutant, T3SS⁻ *cbsA*⁻ double mutant, T3SS⁻ *cbsA*⁻ + pHM1 (empty vector control), T3SS⁻ *cbsA*⁻ + pHM1::*cbsA* (Wt complemented clone), T3SS⁻ *cbsA*⁻ + pHM1::D131A*cbsA* and BXO43 (Wt). The leaves were subsequently treated to remove chlorophyll, stained with aniline blue and visualized under an epifluorescence microscope. Bright spots in the images are the callose deposits. (B) The average numbers of callose spots from at least four leaves and three to four different viewing areas in each experiment were plotted. Error bars represent standard deviation (SD). A Student's two-tailed *t*-test for independent means was performed in pairwise combinations for all the values. Values with the same letter (either a or b) are not significantly different at $P < 0.05$. Similar results were obtained in independent experiments.

cleavage (Vuong and Wilson, 2009; Wu *et al.*, 2013). Interestingly, the crystal structure of the analogous mutant protein D175A Cel6A of *T. reesei* showed the presence of an open active site, which is a characteristic feature of an endoglucanase, as a result of the large conformational change of the N-terminal loop (172–182) harbouring the residue (Koivula *et al.*, 2002). A similar loop conformational change can be expected even in the D131A CbsA mutant of *Xoo*, generating a wider active site, which can explain its endo mode of activity.

The introduction of the D131A *cbsA* clone into the *cbsA* mutant background does not restore, even partially, the virulence deficiency of the *cbsA* mutant. This is in contrast with the observation that the introduction of the Wt *cbsA* gene into the *cbsA* mutant background results in partial restoration of the virulence deficiency of the mutant. Full complementation is not observed, we believe, because the complementing plasmid is unstable during growth within rice leaves (Tayi and Sonti, unpublished results). The endoglucanase activity of the D131A CbsA mutant does not appear to be a substitute for the Wt activity of the protein in promoting virulence on rice. It seems likely that efficient hydrolysis of host cell walls during bacterial growth within rice xylem vessels (the tissue compartment in which the pathogen multiplies) is not possible without the exoglucanase activity of the CbsA protein. Intriguingly, the D131A mutant shows weaker virulence than the cbsA null mutant. One possible explanation for this observation is that *Xoo*-secreted plant CWDEs (such as cellulases, xylanases, esterases, pectinases, etc.) may act in a coordinated manner, although we do not have specific evidence for this. We believe that D131A CbsA may be competing with ClsA for substrate and that, *in vivo*, the products of D131A CbsA action are not as good substrates for the other CWDEs as those produced by the action of ClsA. Thus, the presence of D131A CbsA would inhibit the effectiveness of the other CWDEs, making the *cbsA* mutant strain carrying D131A show weaker virulence than the mutant alone.

Interestingly, the purified D131A CbsA protein is as efficient in inducing defence responses (callose deposition and programmed cell death) in rice tissues as Wt CbsA. In addition, the D131A CbsA protein is as good as the Wt CbsA protein at rescuing the inability of the T3SS$^-$ *cbsA*$^-$ mutant to induce rice innate immune responses. This indicates that, *in vivo*, the D131A CbsA mutant protein can substitute for the Wt protein in eliciting rice innate immune responses during infection. In the majority of cases, the ability of a CWDE to elicit host immune responses comes from its activity on the host cell wall and the release of cell wall degradation products which are recognized as DAMPs (damage-associated molecular patterns) by the host immune system. For instance, in the case of a secreted esterase LipA of *Xoo*, the biochemically inactive enzyme S95A LipA is deficient in inducing rice defence responses (Aparna *et al.*, 2009). However, there are examples wherein some surface structural motif of the CWDE is recognized as a PAMP (pathogen-associated molecular pattern) for the induction of immune responses in the host, and the enzymatic activity of the protein is not required for this purpose. For example, ethylene-inducing xylanase from *T. reesei* and cellulase from *Rhizoctonia solani* have been shown to be inducers of host defence responses without the requirement of any enzymatic activity (Enkerli *et al.*, 1999; Ma *et al.*, 2015; Ron and Avni, 2004).

We have mutated a few other predicted key catalytic residues, such as D180, S137 and Y125, to alanine, but none of these mutations result in a complete loss of biochemical activity. The D226A S232A Cel6B mutant of *T. fusca* exhibits complete loss of activity, but the analogous mutant of CbsA (D131A S137A) is not expressed in *Xoo*. Therefore, at the moment, we are unable to determine whether CbsA is a PAMP or a DAMP.

CbsA also shows a distinct structural feature in the form of two additional loops found only in bacterial CBHs. As these loops are not present in proximity to the active sites, their role in catalytic activity can be ruled out. CbsA also has a fibronectin domain at its C-terminal end that is not required for biochemical activity as it is missing from the secreted protein. The carbohydrate-binding domains of GHs are the counterparts of the fibronectin domain, and have a well-established role in binding to crystalline substrates and increasing the efficiency of catalytic domains (Kataeva *et al.*, 2002; Nakamura *et al.*, 2016). In addition, a nine-residue loop region from the fibronectin-like domain of a pectate lyase PelL of *Dickeya dadantii* has been reported to be involved in the control of the secretion of the protein via the Type 2 secretion system by interacting with the secretion system components (Pineau *et al.*, 2014). The specific roles of the fibronectin domain and bacterial-specific loops of CbsA in the virulence of *Xoo* are being investigated.

EXPERIMENTAL PROCEDURES

Bacterial strains, plasmids, primers and culture media used

The bacterial strains and plasmids used in this study are listed in Table 2. The primers used in this study are listed in Table S2 (see Supporting Information). *Xoo* strains were grown at 28 °C in peptone sucrose (PS) medium. *Escherichia coli* strains were grown in Luria–Bertani (LB) medium at 37 °C. The *Xoo* single crossovers obtained in the process of generating the deletion mutant of *Xoo cbsA* were selected and grown on nutrient agar and nutrient broth medium. The concentrations of antibiotics used were as follows: rifampicin (Rf), 50 μg/mL; ampicillin (Ap), 50 μg/mL; spectinomycin (Sp), 50 μg/mL; kanamycin (Km), 25 μg/mL for *E. coli* and 15 μg/mL for *Xoo*.

Molecular biology and microbiology techniques

Genomic DNA isolation was performed as described in Leach *et al.* (1990). For the amplification of the Wt *cbsA* gene and the D131A version of *cbsA*, high-fidelity Phusion polymerase (Finnzymes, Waltham, MA, USA) was used, and Taq polymerase from KAPA Biosystems (Boston, MA,

Table 2 List of bacterial strains and plasmids used in this study.

Bacterial strain/plasmid	Relevant characteristic(s)	Reference/source
Escherichia coli strains		
DH5α	λ^- f80d *lacZ*DM15 D(*lacZYA-argF*) *U169 recA1 endA hsdR17* (r_K^- m_K^-) *supE44 thi-1 gyrA relA1*	Invitrogen, Carlsbad, CA, US
S17-1	RP4-2 Tc::Mu-Km::Tn*7 pro hsdR recA* Tra+ used as mobilizing strain	Simon *et al.* (1983)
Xanthomonas oryzae pv. *oryzae* strains		
BXO1	Wild-type; Indian isolate	Laboratory collection
BXO43	*rif*-2; derivative of BXO1	Laboratory collection
Δ*cbsA*	*rif*-2; derivative of BXO43	This study
Δ*cbsA*/pHM1	Δ*cbsA*/pHM1; *rif*-2; Sp^r derivative of Δ*cbsA*	This study
Δ*cbsA*/pHM1::*cbsA*	Δ*cbsA*/pHM1::*cbsA*; *rif*-2; Sp^r derivative of Δ*cbsA*	This study
Δ*cbsA*/pHM1::D131A*cbsA*	Δ*cbsA*/pHM1::D131A*cbsA*; *rif*-2; Sp^r derivative of Δ*cbsA*	This study
$T3SS^-$	*hrpB6*::*bla rif*-2; HR^-, Ap^r derivative of BXO43	Jha *et al.* (2007)
$T3SS^-$ *cbsA*$^-$	Δ*cbsA*:: *rif*-2; Ap^r derivative of $T3SS^-$	Tayi *et al.* (2016a)
$T3SS^-$ *cbsA*$^-$/pHM1	$T3SS^-$ *cbsA*$^-$/pHM1; *rif-2;* Ap^r, Sp^r; derivative of $T3SS^-$ *cbsA*$^-$	Tayi *et al.* (2016a, b)
$T3SS^-$ *cbsA*$^-$/pHM1::*cbsA*	$T3SS^-$ *cbsA*$^-$/pHM1::*cbsA*; *rif-2;* Ap^r, Sp^r; derivative of $T3SS^-$ *cbsA*$^-$	This study
$T3SS^-$ *cbsA*$^-$/pHM1::D131A*cbsA*	$T3SS^-$ *cbsA*$^-$/pHM1::D131A*cbsA*; *rif-2;* Ap^r, Sp^r; derivative of $T3SS^-$ *cbsA*$^-$	This study
Plasmids		
pK18*mobsacB*	Allelic exchange suicide vector SacB derivative of pK18*mob*; *sacB* Tra^-Mob^+, Km^r does not replicate in *X. oryzae* pv. *oryzae*	Schäfer, Tauch *et al.* (1994)
pTL1	pK18*mobsacB*+1373 bp of A+C fragment of *cbsA* gene	Tayi *et al.* (2016a, b)
pBSKS	Cloning vector; Ap^r	Stratagene
pBSKS Wt CbsA	pBSKS + 1701 bp *cbsA*	This study
pBSKS D131A CbsA	pBSKS + 1701 bp D131A*cbsA*	This study
pHM1	Broad-host-range cosmid vector (13.3 kb); Sp^r	Innes, Hirose *et al.* (1988)
pHM1 Wt CbsA	pHM1 + 1701 bp *cbsA* gene	This study
pHM1 D131A CbsA	pHM1 + 1701 bp D131A*cbsA* gene	This study

US) was used for all screening purposes. Restriction digestions were carried out using Thermo Fischer Scientific (Waltham, MA, US) Fast Digest enzymes. Ligation reactions were carried out using T4 DNA ligase. Plasmids were purified using either a Macherey Nagel (Duren, Germany) plasmid purification kit or by the alkaline lysis method. Gel extraction and polymerase chain reaction (PCR) purifications were carried out using Macherey Nagel gel extraction and PCR clean-up kits. Agarose gel electrophoresis, transformation of *E. coli*, biparental matings and electroporation of plasmids into *Xoo* were performed as described previously (Ray *et al.*, 2000; Subramoni and Sonti, 2005).

Sequencing and analysis

An ABI Prism 3700 automated DNA sequencer (Perkin-Elmer, Foster City, CA, USA) was used to carry out sequencing of DNA and the sequences obtained were analysed using the BLAST algorithm at the National Center for Biotechnology Information database.

CbsA structure solution

The crystal structure of the catalytic domain of CBH (CbsA) from *Xoo* was determined by the molecular replacement method using Cel6B (E3) from *T. fusca* (PDB ID: 4B4H) as the search model. Initial phasing was performed using MOLREP-AUTO MR from the CCP4 suite (Collaborative Computational Project, 1994). The program AUTOBUILD from PHENIX (Adams *et al.*, 2010) was used for initial model building, followed by iterative cycles of manual model building and refinement using COOT (Emsley and Cowtan, 2004) and PHENIX. A strong electron density could be seen in the active site pocket in which we could not fit any sugar molecule unambiguously and hence was not accounted for. Water molecules were included using COOT, guided by $2F_o–F_c$ and $F_o–F_c$ maps. The final model contains 424 amino acids and 474 water molecules. The data collection and refinement statistics are given in Table 1.

Generation of in-frame deletion *cbsA* mutant of *Xoo*

To generate an in-frame deletion in the *cbsA* gene of *Xoo*, a recombinant plasmid pTL1 (pk18*mobsacB* with in frame-deleted *cbsA* fragment), generated in an earlier study (Tayi *et al.*, 2016a), was used. The plasmid pTL1 was transformed into S17-1 (Simon *et al.*, 1983). Biparental matings were then set up between the S17-1 *E. coli* cells containing pTL1 and Wt *Xoo* (BXO43). BXO43 cells which have integrated the plasmid at the correct locus in the genome were selected by kanamycin resistance and confirmed

by PCR using a pair of primers flanking the *cbsA* gene (Table S2). Confirmed single recombinants were grown in nutrient broth without kanamycin and plated on 1% potato sucrose agar (PSA) plates to isolate cells which had undergone a second recombination event. Double recombinants which include both mutants and Wt cells were screened and the in frame deletion of the *cbsA* gene in the mutants was confirmed as described previously (Tayi *et al.*, 2016a).

Generation of D131A CbsA mutant

The *cbsA* gene was PCR amplified from the genome of the BXO43 strain of *Xoo* (Wt), with primers having *Hind*III and *Eco*RI restriction sites at the 5′ and 3′ ends, respectively (Table S2). The amplified gene was restriction digested with these enzymes to obtain a product with sticky ends. We used the pBSKS (Stratagene, San Diego, CA, US) plasmid as a shuttle vector for gene amplification and site-directed mutagenesis studies. Plasmid pBSKS was double digested (with the same enzymes) and used for ligation with the doubly digested *cbsA* gene product. The ligation product was transformed into DH5α cells and the vector–gene construct was used for site-directed mutagenesis studies. The D131A mutant was generated by PCR amplification using the primers listed in Table S2, followed by 30 min of digestion with *Dpn*I to digest the Wt *cbsA*-pBSKS constructs. The mutations were then confirmed by DNA sequencing. The positive constructs were then again digested with *Hind*III and *Eco*RI, and ligated in *Hind*III–*Eco*RI-digested pHM1 vector. These pHM1-*CbsA* mutant constructs were transformed into DH5α cells. The plasmids were purified from these cultures and used for electroporation into a *Xoo* strain which has an in-frame deletion of the *cbsA* gene. This strain was used further for purification of the D131A CbsA mutant protein.

Enzyme purification

Wt *Xoo* (BXO43) was used for purification of the CbsA and ClsA proteins. D131A CbsA protein was purified from a *cbsA*$^-$ mutant strain expressing D131A CbsA from the pHM1 cosmid. The strains were grown until saturation. The extracellular culture supernatant was obtained by pelleting the cells at 4°C, 9.8 Kg, for 20 min. Secreted proteins in the culture supernatant were precipitated using ammonium sulfate (55% saturation) and the pellet was dissolved in 0.01 M potassium phosphate buffer, pH 6.0. Excess salt was removed by extensive dialysis against the same buffer. Proteins in the dialysed sample were separated into various fractions by cation exchange chromatography using a MONO S column with a linear gradient of 0.01 M potassium phosphate buffer, pH 6.0 (Buffer A), to 0.01 M potassium phosphate buffer, pH 6.0, and 1 M NaCl (Buffer B). Subsequently, using gel filtration chromatography (Superdex 200, GE Healthcare, Chicago, Illinois, US), the Wt CbsA and D131A CbsA proteins were purified to homogeneity in 0.02 M Tris-Cl, pH 8.0, and 0.02 M NaCl. The purity of the proteins was confirmed by sodium dodecylsulfate-polyacrylamide gel electrophoresis (SDS-PAGE).

CMC plate assay

A 1.2% agarose suspension containing 0.1% of CMC was poured into Petri plates. After solidification, wells were cut out and filled with either the enzyme or buffer. Following incubation at 28°C for 36–48 h, the plates were stained with 1% Congo red solution and then destained with 1 M NaCl. A zone of clearance around the well indicates cellulase activity.

Thin layer chromatography

Ten micrograms of the oligomeric substrates cellobiose, cellotriose, cellotetraose, cellopentaose and cellohexaose were hydrolysed to completion by incubation with 1 μM of any one of the following: Wt CbsA, D131A CbsA or ClsA enzyme. Similarly, 100 μg of CMC was treated with 1 μM of enzyme for 16 h at 37°C. Hydrolysis products were separated on 0.2-mm aluminium sheet silica gel 60 plates (Merck, Kenilworth, NJ, US) with a butanol, acetic acid and water mixture (2 : 1 : 1) as eluent. Sugars were detected by dipping the plates in a freshly prepared solution containing 10% sulfuric acid and 0.1% methanolic orcinol (1 : 1), followed by heating the plates at 80°C until the colour developed.

Estimation of reducing sugars

One millilitre of a reaction mixture containing 0.5 mL of 2% CMC solution and 0.2 μM of either Wt CbsA or D131A CbsA was incubated for 4 h at 37°C. To stop the reaction, 3 mL of 3,5-dinitro salicylic acid (DNS) solution was added to the complete reaction mixture, followed by boiling. The absorbance of the samples and glucose standards was measured at 540 nm in a spectrophotometer and the specific activity of the enzyme was calculated.

Viscosity measurements

Five millilitres of 2% (w/v) solution of CMC were hydrolysed with 0.2 μM of ClsA, Wt CbsA or D131A CbsA in a 10-mL reaction. The flow time of the reaction mixture was determined at intervals of 2, 4 and 6 h in a kinematic viscosity bath (Cannon in USA, State College, PA, US) at 37°C. The kinematic viscosity was calculated by multiplying the correction value specific for the vessel with the flow time of the sample.

Virulence assay

Wt *Xoo* (BXO43), *cbsA*$^-$ mutant, *cbsA*$^-$ mutant expressing either the Wt CbsA protein or D131A CbsA protein from pHM1 vector and *cbsA*$^-$ mutant carrying the empty pHM1 vector were grown in PS broth with appropriate antibiotics. The bacterial cells were pelleted by centrifugation at 2.4 Kg for 5 min at room temperature, washed and resuspended in sterile Milli Q (MQ) water. Forty to 45-day-old Taichung Native-1 (TN-1) rice leaf tips were cut with surgical scissors dipped in a bacterial suspension with an optical density at 600 nm (OD_{600}) of 1. Lesion lengths were measured at 20 days post-inoculation.

Callose deposition assay

TN-1 rice seedlings (about 10–15 days old) were infiltrated with buffer (10 mM phosphate buffer, pH 6.0), Wt CbsA or D131A CbsA proteins (of 0.1 mg/mL) or cultures of the *Xoo* strains Wt (BXO43), T3SS$^-$, T3SS$^-$ *cbsA*$^-$, T3SS$^-$ *cbsA*$^-$ + pHM1 (empty vector control strain), T3SS$^-$ *cbsA*$^-$ + pHM1::Wt*cbsA* and T3SS$^-$ *cbsA*$^-$ + pHM1::D131A*cbsA* with $OD_{600} = 1.0$ using a needleless syringe. Sixteen hours later, the infiltrated zones (approximately 1 cm in length) were cut from the leaves and pigments were removed by heating at 60°C with alcohol. Subsequently, the

samples were stained with 0.5% aniline blue solution prepared in 150 mM K_2HPO4 and analysed under an epifluorescence microscope using a blue filter and ×10 objective.

Cell death assay

TN-1 rice seeds were surface sterilized and germinated on sterile filter paper overlaid on 0.5% agar in Petri dishes; 1–2-cm-long root tips were excised from the seedlings and treated with buffer (10 mM phosphate buffer, pH 6.0), Wt CbsA or D131A CbsA protein (500 μL of 0.5 mg/mL). After incubation for 16–18 h, the roots were washed with sterile MQ water and stained with PI. The PI-stained roots were mounted in 50% glycerol on glass slides. The PI internalization in root cells was further detected in an LSM-510 Meta confocal microscope (Carl Zeiss, Jena, Germany) under a 63× oil immersion objective using an He–Ne laser excited at 543 nm. One-micrometre-thick longitudinal optical sections were captured and further projected to obtain an image of 2–3 μm total thickness. All images were analysed using LSM software.

ACKNOWLEDGEMENTS

We acknowledge the help received from Amit Rajak, Dr Prabhavathi Devi and Dr R. B. N. Prasad of the Lipid Research Facility of the CSIR-Indian Institute of Chemical Technology in carrying out the viscosity experiments. LT, SK and RN acknowledge fellowships from the Indian Council of Medical Research, the University Grants Commission and the Council of Scientific and Industrial Research, respectively. This work was supported by the XIIth five year plan project, Plant–Microbe and Soil Interactions (BSC0117), of the Council of Scientific and Industrial Research. RVS and RS were also supported by a J. C. Bose Fellowship from the Department of Science and Technology, Government of India. The authors have no conflicts of interest to declare.

REFERENCES

Adams, P.D., Afonine, P.V., Bunkóczi, G., Chen, V.B., Davis, I.W., Echols, N., Headd, J.J., Hung, L.-W., Kapral, G.J., Grosse-Kunstleve, R.W., McCoy, A.J., Moriarty, N.W., Oeffner, R., Read, R.J., Richardson, D.C., Richardson, J.S., Terwilliger, T.C. and Zwart, P.H. (2010) PHENIX: a comprehensive Python-based system for macromolecular structure solution. *Acta Crystallogr. D: Biol. Crystallogr.* **66**, 213–221.

Aparna, G., Chatterjee, A., Sonti, R.V. and Sankaranarayanan, R. (2009) A cell wall-degrading esterase of *Xanthomonas oryzae* requires a unique substrate recognition module for pathogenesis on rice. *Plant Cell*, **21**, 1860–1873.

Cantarel, B.L., Coutinho, P.M., Rancurel, C., Bernard, T., Lombard, V. and Henrissat, B. (2009) The Carbohydrate-Active EnZymes database (CAZy): an expert resource for glycogenomics. *Nucleic Acids Res.* **37**, D233–D238.

Collaborative Computational Project. (1994) The CCP4 suite: programs for protein crystallography. *Acta Crystallogr. D: Biol. Crystallogr.* **50**, 760.

Davies, G.J., Brzozowski, A.M., Dauter, M., Varrot, A. and Schülein, M. (2000) Structure and function of *Humicola insolens* family 6 cellulases: structure of the endoglucanase, Cel6B, at 1.6 Å resolution. *Biochem. J.* **348**, 201–207.

Emsley, P. and Cowtan, K. (2004) Coot: model-building tools for molecular graphics. *Acta Crystallogr. D: Biol. Crystallogr.* **60**, 2126–2132.

Enkerli, J., Felix, G. and Boller, T. (1999) The enzymatic activity of fungal xylanase is not necessary for its elicitor activity. *Plant Physiol.* **121**, 391–398.

Gough, C.L., Dow, J.M., Barber, C.E. and Daniels, M.J. (1988) Cloning of two endoglucanase genes of *Xanthomonas campestris* pv. *campestris*: analysis of the role of the major endoglucanase in pathogenesis. *Mol. Plant–Microbe Interact.* **1**, 275–281.

Henrissat, B. (1991) A classification of glycosyl hydrolases based on amino acid sequence similarities. *Biochem. J.* **280**, 309–316.

Hon, D.N.-S. (1994) Cellulose: a random walk along its historical path. *Cellulose*, **1**, 1–25.

Innes, R.W., Hirose, M.A. and Kuempel, P.L. (1988) Induction of nitrogen-fixing nodules on clover requires only 32 kilobase pairs of DNA from the Rhizobium trifolii symbiosis plasmid. *J. Bacteriol.* **170**, 3793–3802.

Jha, G., Rajeshwari, R. and Sonti, R.V. (2007) Functional interplay between two *Xanthomonas oryzae pv. oryzae* secretion systems in modulating virulence on rice. *Mol. Plant–Microbe Interact.* **20**, 31–40.

Kataeva, I.A., Seidel, R.D., Shah, A., West, L.T., Li, X.-L. and Ljungdahl, L.G. (2002) The fibronectin type 3-like repeat from the *Clostridium thermocellum* cellobiohydrolase CbhA promotes hydrolysis of cellulose by modifying its surface. *Appl. Environ. Microbiol.* **68**, 4292–4300.

Koivula, A., Reinikainen, T., Ruohonen, L., Valkeajärvi, A., Claeyssens, M., Teleman, O., Kleywegt, G.J., Szardenings, M., Rouvinen, J., Jones, T.A. and Teeri, T.T. (1996) The active site of *Trichoderma reesei* cellobiohydrolase II: the role of tyrosine 169. *Protein Eng.* **9**, 691–699.

Koivula, A., Ruohonen, L., Wohlfahrt, G., Reinikainen, T., Teeri, T.T., Piens, K., Claeyssens, M., Weber, M., Vasella, A., Becker, D., Sinnott, M.L., Zou, J.-Y., Kleywegt, G.J., Szardenings, M., Ståhlberg, J. and Jones, T.A. (2002) The active site of cellobiohydrolase Cel6A from *Trichoderma reesei*: the roles of aspartic acids D221 and D175. *J. Am. Chem. Soc.* **124**, 10 015–10 024.

Kumar, S., Haque, A.S., Jha, G., Sonti, R.V. and Sankaranarayanan, R. (2012) Crystallization and preliminary crystallographic studies of CbsA, a secretory exoglucanase from *Xanthomonas oryzae pv. oryzae*. *Acta Crystallogr. Sect. F: Struct. Biol. Cryst. Commun.* **68**, 1191–1194.

Leach, J.E., White, F.F., Rhoads, M.L., and Leung, H. (1990) A repetitive DNA sequence differentiates Xanthomonas campestris pv. oryzae from other pathovars of X. campestris. *Mol. Plant-Microbe Interact.* **3**, 238–246.

Liu, Y., Yoshida, M., Kurakata, Y., Miyazaki, T., Igarashi, K., Samejima, M., Fukuda, K., Nishikawa, A. and Tonozuka, T. (2010) Crystal structure of a glycoside hydrolase family 6 enzyme, CcCel6C, a cellulase constitutively produced by *Coprinopsis cinerea*. *FEBS J.* **277**, 1532–1542.

Ma, Y., Han, C., Chen, J., Li, H., He, K., Liu, A. and Li, D. (2015) Fungal cellulase is an elicitor but its enzymatic activity is not required for its elicitor activity. *Mol. Plant Pathol.* **16**, 14–26.

Mayes, H.B., Knott, B.C., Crowley, M.F., Broadbelt, L.J., Ståhlberg, J. and Beckham, G.T. (2016) Who's on base? Revealing the catalytic mechanism of inverting family 6 glycoside hydrolases. *Chem. Sci.* **7**, 5955–5968.

Nakamura, A., Tasaki, T., Ishiwata, D., Yamamoto, M., Okuni, Y., Visootsat, A., Maximilien, M., Noji, H., Uchiyama, T., Samejima, M., Igarashi, K. and Iino, R. (2016) Single-molecule imaging analysis of binding, processive movement, and dissociation of cellobiohydrolase *Trichoderma reesei* Cel6A and its domains on crystalline cellulose. *J. Biol. Chem.* **291**, 22 404–22 413.

Pineau, C., Guschinskaya, N., Robert, X., Gouet, P., Ballut, L. and Shevchik, V.E. (2014) Substrate recognition by the bacterial type II secretion system: more than a simple interaction. *Mol. Microbiol.* **94**, 126–140.

Rajeshwari, R., Jha, G. and Sonti, R.V. (2005) Role of an in planta-expressed xylanase of *Xanthomonas oryzae pv. oryzae* in promoting virulence on rice. *Mol. Plant–Microbe Interact.* **18**, 830–837.

Ray, S.K., Rajeshwari, R. and Sonti, R.V. (2000) Mutants of *Xanthomonas oryzae pv. oryzae* deficient in general secretory pathway are virulence deficient and unable to secrete xylanase. *Mol. Plant–Microbe Interact.* **13**, 394–401.

Roberts, D., Denny, T. and Schell, M. (1988) Cloning of the egl gene of *Pseudomonas solanacearum* and analysis of its role in phytopathogenicity. *J. Bacteriol.* **170**, 1445–1451.

Ron, M. and Avni, A. (2004) The receptor for the fungal elicitor ethylene-inducing xylanase is a member of a resistance-like gene family in tomato. *Plant Cell*, **16**, 1604–1615.

Rouvinen, J., Bergfors, T., Teeri, T., Knowles, J. and Jones, T. (1990) Three-dimensional structure of cellobiohydrolase II from *Trichoderma reesei*. *Science*, **249**, 380–386.

Ryan, R.P., Vorhölter, F.-J., Potnis, N., Jones, J.B., Van Sluys, M.-A., Bogdanove, A.J. and Dow, J.M. (2011) Pathogenomics of *Xanthomonas*: understanding bacterium–plant interactions. *Nat. Rev. Microbiol.* **9**, 344–355.

Sandgren, M., Wu, M., Karkehabadi, S., Mitchinson, C., Kelemen, B.R., Larenas, E.A., Ståhlberg, J. and Hansson, H. (2013) The structure of a bacterial cellobiohydrolase: the catalytic core of the *Thermobifida fusca* family GH6 cellobiohydrolase Cel6B. *J. Mol. Biol.* **425**, 622–635.

Sato, C., Oka, N., Nabeta, K. and Matsuura, H. (2011) Cellulase applied to the leaves of sweet pepper (*Capsicum annuum* L. var. *grossum*) upregulates the production of salicylic and azelaic acids. *Biosci. Biotechnol. Biochem.* **75**, 761–763.

Schafer, A., Tauch, A., Jager, W., Kalinowski, J., Thierbach, G. and Puhler, A. (1994) Small mobilizable multi-purpose cloning vectors derived from the Escherichia coli plasmids pK18 and pK19: selection of defined deletions in the chromosome of Corynebacterium glutamicum. *Gene.* **145**, 69–73.

Simon, R., Priefer, U. and Pühler, A. (1983) A broad host range mobilization system for in vivo genetic engineering: transposon mutagenesis in gram negative bacteria. *Nat. Biotechnol.* **1**, 784–791.

Subramoni, S. and Sonti, R.V. (2005) Growth deficiency of a *Xanthomonas oryzae pv. oryzae* fur mutant in rice leaves is rescued by ascorbic acid supplementation. *Mol. Plant–Microbe Interact.* **18**, 644–651.

Tamura, M., Miyazaki, T., Tanaka, Y., Yoshida, M., Nishikawa, A. and Tonozuka, T. (2012) Comparison of the structural changes in two cellobiohydrolases, CcCel6A and CcCel6C, from *Coprinopsis cinerea*–a tweezer-like motion in the structure of CcCel6C. *FEBS J.* **279**, 1871–1882.

Tayi, L., Maku, R., Patel, H.K. and Sonti, R. (2016a) Action of multiple cell wall degrading enzymes is required for elicitation of innate immune responses during *Xanthomonas oryzae pv. oryzae* infection in rice. *Mol. Plant–Microbe Interact.* **29**, 599–608.

Tayi, L., Maku, R.V., Patel, H.K. and Sonti, R.V. (2016b) Identification of pectin degrading enzymes secreted by *Xanthomonas oryzae pv. oryzae* and determination of their role in virulence on rice. *PLoS One*, **11**, e0166396.

Teeri, T.T. (1997) Crystalline cellulose degradation: new insight into the function of cellobiohydrolases. *Trends Biotechnol.* **15**, 160–167.

Teeri, T., Koivula, A., Linder, M., Wohlfahrt, G., Divne, C. and Jones, T. (1998) *Trichoderma reesei* cellobiohydrolases: why so efficient on crystalline cellulose? *Biochem. Soc. Trans.* **26**, 173–178.

Thompson, A.J., Heu, T., Shaghasi, T., Benyamino, R., Jones, A., Friis, E.P., Wilson, K.S. and Davies, G.J. (2012) Structure of the catalytic core module of the *Chaetomium thermophilum* family GH6 cellobiohydrolase Cel6A. *Acta Crystallogr. D: Biol. Crystallogr.* **68**, 875–882.

Varrot, A., Hastrup, S., Schülein, M. and Davies, G.J. (1999a) Crystal structure of the catalytic core domain of the family 6 cellobiohydrolase II, Cel6A, from *Humicola insolens*, at 1.92 Å resolution. *Biochem. J.* **337**, 297–304.

Varrot, A., Schülein, M. and Davies, G.J. (1999b) Structural changes of the active site tunnel of *Humicola insolens* cellobiohydrolase, Cel6A, upon oligosaccharide binding. *Biochemistry*, **38**, 8884–8891.

Varrot, A., Frandsen, T.P., von Ossowski, I., Boyer, V., Cottaz, S., Driguez, H., Schülein, M. and Davies, G.J. (2003) Structural basis for ligand binding and processivity in cellobiohydrolase Cel6A from *Humicola insolens*. *Structure*, **11**, 855–864.

Vuong, T.V. and Wilson, D.B. (2009) The absence of an identifiable single catalytic base residue in *Thermobifida fusca* exocellulase Cel6B. *FEBS J.* **276**, 3837–3845.

Wu, M., Bu, L., Vuong, T.V., Wilson, D.B., Crowley, M.F., Sandgren, M., Ståhlberg, J., Beckham, G.T. and Hansson, H. (2013) Loop motions important to product expulsion in the *Thermobifida fusca* glycoside hydrolase family 6 cellobiohydrolase from structural and computational studies. *J. Biol. Chem.* **288**, 33 107–33 117.

Xia, T., Li, Y., Sun, D., Zhuo, T., Fan, X. and Zou, H. (2016) Identification of an extracellular endoglucanase that is required for full virulence in *Xanthomonas citri* subsp. *citri*. *PLoS One*, **11**, e0151017.

Zou, J-Y., Kleywegt, G.J., Ståhlberg, J., Driguez, H., Nerinckx, W., Claeyssens, M., Koivula, A., Teeri, T.T. and Jones, T.A. (1999) Crystallographic evidence for substrate ring distortion and protein conformational changes during catalysis in cellobiohydrolase Ce16A from *Trichoderma reesei*. *Structure*, **7**, 1035–1045.

SUPPORTING INFORMATION

Additional Supporting Information may be found in the online version of this article at the publisher's website:

Fig. S1 The conserved tryptophans lining the active site tunnel. Tryptophans around the active site tunnel which help to anchor the substrate by virtue of π–π interactions with the sugar rings are shown with sticks. (Ligand was modelled from PDB ID: 4B4F.)

Table S1 Specific activity of wild-type (Wt) CbsA and D131A CbsA.

Table S2 List of primers used in this study.